$K\alpha$ x-ray satellite distribution of Ar produced in heavy ion collisions

V. Horvat, R. L. Watson, and Y. Peng

Spectra of $K\alpha$ x rays emitted from Ar gas at atmospheric pressure under bombardment by 10 MeV/amu heavy ions (atomic number Z_1 = 6 to 79) were measured in high resolution using a curved crystal spectrometer. The results are shown in Figure 1. Energies of the $K\alpha_{1,2}$ and $K\beta_1$ diagram transitions are indicated by the vertical dashed lines. The $K\alpha_{1,2}$ peak includes unresolved contributions of $2p \rightarrow 1s$ transitions from ions with a single vacancy and $2p \rightarrow 1s$ transitions from ions with additional M-shell vacancies. The former are known as $K\alpha$ diagram transitions, while the latter will be referred to as $K\alpha L^0$ satellites. Additional i spectator vacancies in the L shell give rise to the peaks that are shifted up in energy and, consequently, resolved from each other and from the previously described $K\alpha_{1,2}$ peak. They will be referred to as $K\alpha L^i$ satellite peaks. Most of the $K\alpha L^i$ satellite transitions (i = 0 to 7) are due to K-shell ionization by the projectiles, while most of the diagram transitions are due to secondary K-shell ionization [1,2]. Figure 1 shows that the distribution of $K\alpha$ satellites shifts to higher average values of i as the projectile atomic number increases.

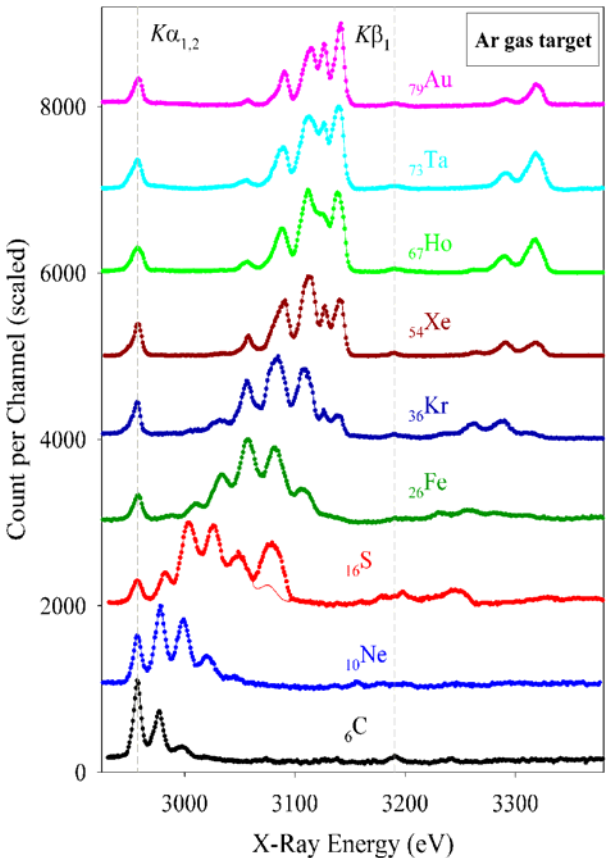

Figure 1. Measured spectra of x rays emitted from Ar gas at the pressure of 1 atm under bombardment by 10 MeV/amu ions (as labeled).

The distribution of M-shell vacancies associated with $K\alpha L^i$ satellite transitions affects the widths and centroids of the corresponding peaks. Typically, this effect is small enough so that the $K\alpha L^i$ satellite peaks still can be resolved from each other, but large enough to obliterate any structure that might arise due to the various ways in which the electronic angular momenta can be coupled (i.e., multiplet splitting), although, in most cases, such a structure cannot be observed due to the complexity of multiplet splitting alone. However, there are two notable exceptions. One corresponds to the case in which i = 0 and the average number of M-shell vacancies is much less than one, while the other corresponds to the case in which i = 7 and the average number of M-shell vacancies is very close to the maximum (i.e., 8 for Ar). In the former case it may be possible to resolve the $K\alpha_{1,2}$ doublet (provided that the resolution of the

spectrometer is adequate, which is not the case here), while in the latter case it may be possible to resolve the $K\alpha L^7$ doublet (which is the case here). The latter effect is obvious in the spectra induced by Kr, Xe, Ho, Ta, and Au projectiles, in which the two $K\alpha L^7$ peaks are prominent.

In the absence of any M-shell electrons, the $K\alpha L^7$ doublet consists of a lower energy peak, corresponding to the $1s2p(^3P)\rightarrow 1s^2(^1S)$ transition, and a higher energy peak, corresponding to the $1s2p(^1P)\rightarrow 1s^2(^1S)$ transition. The predominant contribution to the ^3P peak is expected to originate from the $^3P_1$ state, which should be formed with the same statistical probability as the $^1P_1$ state, but its decay is delayed because $^3P\rightarrow{}^1S$ transitions are spin forbidden. Therefore, there is a larger probability for the ^3P state to decay by non-radiative means, such as collisional quenching. The probability for collisional quenching increases with increasing gas pressure, which leads to the reduction in intensity of the $^3P\rightarrow{}^1S$ peak relative to the $^1P\rightarrow{}^1S$ peak [3].

An additional K vacancy gives rise to peaks that are shifted even higher up in energy. They are referred to as $K^2\alpha L^i$ satellite peaks (or $K\alpha$ hypersatellites). In the case of Ar, $K\alpha$ hypersatellites start somewhere between the $K\alpha L^7$ satellite and the $K\beta_1$ diagram peak. As illustrated by Figure 1, their distribution also shifts to higher average values of i as the projectile atomic number increases. In the spectra induced by C and Ne projectiles, the hypersatellite peaks are buried in the background.

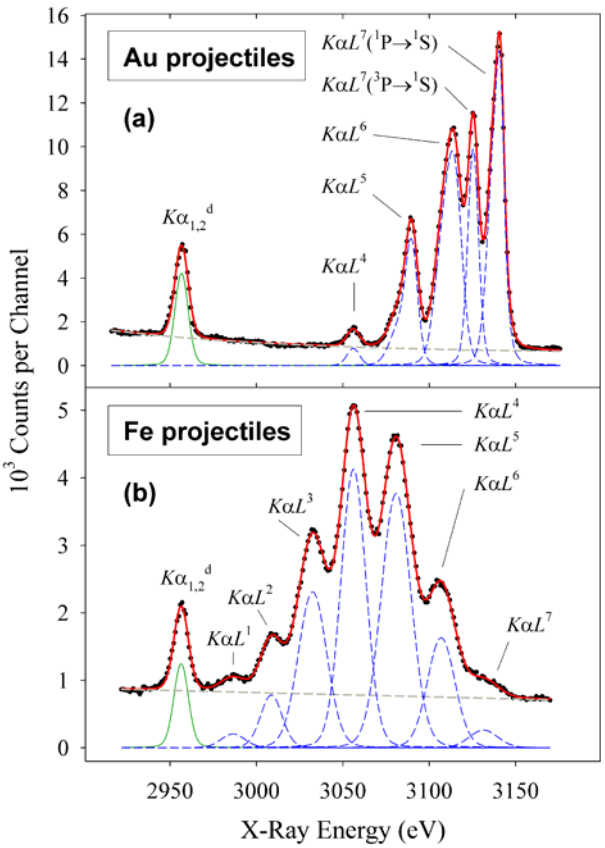

Figure 2. Fitted $K\alpha$ satellite spectra of Ar induced by (a) Au and (b) Fe projectiles at 10 MeV/amu.

The measured x-ray spectrum induced by sulfur ions contains significant contributions from the projectile $K\beta_1$ transitions. Their contribution overlaps with that of the Ar $K\alpha L^5$ satellite. The red circles in Figure 1 show the uncorrected (normalized) spectrum, while the red line shows the spectrum in which the contribution from sulfur $3p\rightarrow 1s$ transitions has been subtracted. Additionally, iron projectile $K\alpha$ x rays from second order diffraction may contribute to the Ar K x-ray spectra in the hypersatellite region. Therefore, the peaks in the Ar $K\alpha$ hypersatellite region were analyzed only for the spectra induced by Kr, Xe, Ho, Ta, and Au projectiles.

The $K\alpha$ satellite and hypersatellite intensity can be described quantitatively in terms of the apparent average fraction of L vacancies (p_L^x), defined as

$$p_L^x = \tfrac{1}{8}\sum_{i=1}^{8}(iI_i)/I_{tot}\ , \qquad (1)$$

where

$$I_{tot} = \sum_{i=0}^{8} I_i \ , \qquad (2)$$

In the expressions above, I_i are the intensities of the $K\alpha L^i$ peaks. For selected cases (listed above), $p_L{}^x$ was also determined from the intensities of $K^2\alpha L^i$ peaks.

Two examples of the fitted $K\alpha$ satellite spectra (those obtained with Au and Fe projectiles) are shown in Figure 2. The measured data points are shown as solid black circles, while the thick solid (red) line represents the overall fit. The background is shown as a thick dashed (gray) line, while the thin solid (green) line outlines the contributions from the diagram x rays. The thin dashed (blue) lines represent the contributions from individual peaks.

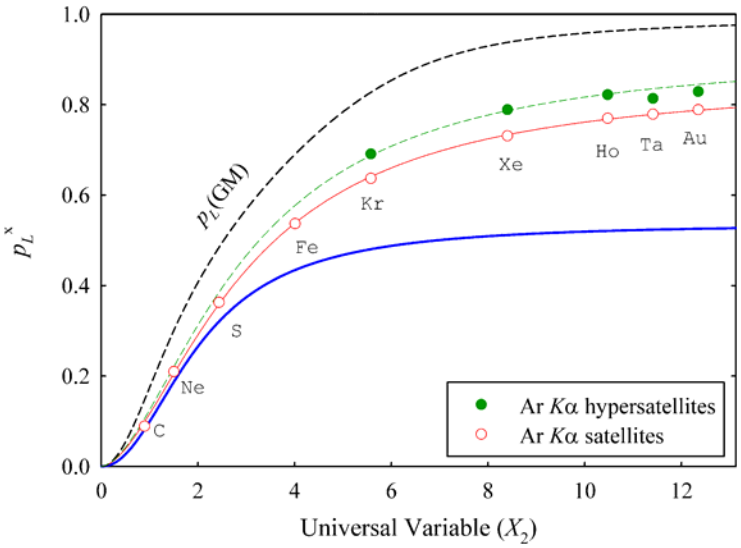

Figure 3. The apparent average fraction of L-shell vacancies at the time of K x-ray emission ($p_L{}^x$) as a function of the universal variable.

The values of $p_L{}^x$ determined using Eqs.(1,2) based on the results from least-squares curve-fitting of the collected spectra are shown in Figure 3, in which the open circles show the results obtained using the intensities of the $K\alpha$ satellite peaks, while the filled circles show those obtained using the intensities of the $K\alpha$ hypersatellite peaks. The thin solid (red) line is the best-fit logistic curve for the "satellite" data points, while the thin dashed (green) line is the best-fit logistic curve for the "hypersatellite" data points. The thick solid (blue) line represents the result from Ref.[4], which was obtained from the satellite peak intensities in measurements with various *solid* targets (atomic numbers Z_2 = 6 to 92). The thick dashed (black) line represents the geometrical model prediction of the average fraction of L vacancies at the time of collision, according to Eq.(21) from Ref.[5].

The magnitude of the difference between the red and the blue curve in Figure 3 at any given value of X_2 is a measure of the (negative) contribution of interatomic transitions to the values of $p_L{}^x$ in solids. Apparently, interatomic transitions play an increasingly significant role as the number of atomic vacancies increases (i.e. when the rate of intraatomic transitions is reduced due to the reduced availability of atomic electrons). Actually, the differences between the red and the blue curves in Figure 3 are more likely to represent lower limits to the contributions from interatomic transitions. This is because projectiles traveling in solids have more inner-shell vacancies than those traveling in gas due to the higher collision frequency. Therefore, ionization of solid targets should initially be enhanced over that of gas targets.

The green curve in Figure 3 shows the results obtained for the *K*α hypersatellites. It lies above the red curve for all values of X_2, which reflects the fact that an increased degree of *K*-shell ionization also leads to an increased degree of *L*-shell ionization. Apparently, collisions between a target atom and a heavy ion at smaller impact parameters (i.e., those that are more likely to result in double *K*-shell ionization) also reduce the *L*-shell electron population more effectively.

[1] R. L. Watson, J. M. Blackadar, and V. Horvat, Phys. Rev. A **60**, 2959 (1999).

[2] V. Horvat and R. L. Watson, J. Phys. B **34**, 777 (2001).

[3] H. F. Beyer, R. Mann, and F. Folkmann, J. Phys. B **14**, L377 (1981), H. F. Beyer, R. Mann, and F. Folkmann, J. Phys. B **15**, 1083 (1982).

[4] V. Horvat, R. L. Watson, and Y. Peng, Phys. Rev. A **74**, 022718 (2006).

[5] B. Sulik, I. Kadar, S. Ricz, D. Varga, J. Vegh, G. Hock, and D. Berenyi, Nucl. Instrum. Methods Phys. Res. **B28**, 509 (1987).